Talanta 99 (2012) 387–393

Contents lists available at SciVerse ScienceDirect

Talanta

journal homepage: www.elsevier.com/locate/talanta

Near infrared dye indocyanine green doped silica nanoparticles for biological imaging

Bo Quan [a], Kihwan Choi [a], Young-Hwa Kim [b], Keon Wook Kang [b], Doo Soo Chung [a,*]

[a] Department of Chemistry, Seoul National University, Seoul 151-747, South Korea
[b] Department of Nuclear Medicine, Seoul National University, Seoul 110-744, South Korea

ARTICLE INFO

Article history:
Received 8 February 2012
Received in revised form
30 May 2012
Accepted 31 May 2012
Available online 13 June 2012

Keywords:
Indocyanine green (ICG)
Near infrared (NIR)
Silica nanoparticles
Polyethylenimine (PEI)

ABSTRACT

Indocyanine green (ICG) is an FDA-approved near infrared (NIR) fluorescent dye used in clinical imaging. However, its applications remain limited due to its short half-life, nonspecific plasma binding, optical instability, and poor aqueous stability. Dye doped silica nanoparticles provide an effective barrier in keeping the dye away from the surrounding environment, but ICG cannot be encapsulated into silica easily by conventional methods. In this study, ICG molecules ion-paired with a cationic polymer polyethylenimine (PEI) were successfully encapsulated into a silica matrix to form ICG doped silica nanoparticles by using the Stöber method. Pairing with PEI reduced self-quenching of fluorescence by preventing the aggregation of ICG molecules in silica nanoparticles. Dye leakage was also reduced to the level of 3–6% loss in 5 days. NIR fluorescence images of ICG doped silica NPs below a 2.0 cm thick porcine muscle sample illuminated by NIR light were obtained.

1. Introduction

Since near infrared (NIR) light passes readily through biological tissues and causes little damage [1], NIR fluorescence materials are well suited for bioimaging in organisms and clinical diagnostic imaging in deep tissues [2–5]. Indocyanine green (ICG) is an NIR organic dye approved by the US Food and Drug Administration for clinical use [6,7]. Since it has a low toxicity [8] and is injectable [9], ICG has a number of clinical uses such as photodynamic therapy [10–12], optical angiography [13] and guiding sentinel node biopsy [14]. However, more extensive in vivo and in vitro applications of ICG in bioimaging are rather limited. ICG has a low fluorescence quantum yield in aqueous solutions because of self-quenching [15,16] and it is inadequate for use in physiologically relevant aqueous solutions [17–19]. ICG nonspecifically binds to plasma proteins, such as albumin, globulins, and lipoproteins [18,20,21], and is quickly removed from the circulatory system by the action of the liver [22]. Its initial half-life is only about 3–4 min. In addition, interference of targeting and image analysis by photobleaching may occur [18,23,24]. For example, a solution of ICG was injected into a human liver, approximately 8 mm below the liver surface, for the detection of tumors [25]. However, due to the rapid elimination of ICG from the body after intravenous administration [26], as much as 5 mL of 5 mg/mL solution of ICG had to be used. In order to solve these problems, ICG containing (as much as 29 wt%) poly(lactic-co-glycolic acid) (PLGA) nanoparticles (NPs) were developed to improve the stability of ICG [27–30]. Nanoparticle-assembled capsules (NACs) containing ICG were also developed to reduce the leakage of the dye [31,32]. The sizes of the capsules were limited to the range 60–2000 nm, with ICG content ranging from 0.4 to 23 wt%.

Dye doped silica NPs protect the dye from photobleaching and photodegradation [33]. The silica surface also enables easy and flexible surface treatments. In addition, silica is considered to be a biocompatible material and can be used in physiologically relevant solutions [34]. The US Food and Drug Administration listed silica as "generally recognized as safe" (GRAS) [35]. However, studies showed that the cytotoxicity of silica NPs depended on the NP sizes [36–38]. For example, silica NPs with diameter size below 50 nm reduced in vitro cell viability. In our previous research [39], rhodamine B isothiocyanate (RITC) doped silica NPs of 75 nm in diameter were small enough to pass freely through lymphatic channels, but remained trapped in lymph nodes. To the best of our knowledge, however, ICG doped silica NPs taking advantage of the high transmittance of NIR through tissue have not been reported yet, probably due to the electrostatic repulsions between anionic ICG molecules and the negative silanoate groups of silica.

In this report, ICG molecules were ion-paired with a cationic polymer polyethylenimine (PEI) to be encapsulated by a silica layer using the Stöber method [40,41]. The resulting ICG doped

* Corresponding author. Tel.: +82 2 880 8130; fax: +82 2 877 3025.
E-mail address: dschung@snu.ac.kr (D.S. Chung).

0039-9140/$ - see front matter © 2012 Elsevier B.V. All rights reserved.
http://dx.doi.org/10.1016/j.talanta.2012.05.069

silica NPs had diameters in the range 50–200 nm, which are adequate for various in vivo experiments [42,43]. After the ICG molecules were paired with PEI, dye loss through the silica layer was significantly reduced and fluorescence self-quenching was also reduced. By illuminating a 2.0 cm thick porcine muscle sample with NIR light (710–760 nm), NIR fluorescence (780–950 nm) images of ICG doped silica NPs below the sample were obtained.

2. Experimental

2.1. Materials

ICG, RITC, dimethyl sulfoxide (DMSO), 3-(aminopropyl) triethoxysilane (APTS), and phosphate buffered saline (PBS, pH 7.4) were obtained from Sigma (St. Louis, MO, USA). A 50 wt% PEI of average M_n 60,000 (PEI_{60000}) solution was from Supelco (Bellefonte, PA, USA). A 50 wt% PEI of average M_n 1200 (PEI_{1200}), M_n 10,000 (PEI_{10000}) solution, ethanol, tetraethyl orthosilicate (TEOS), and 29 wt% aqueous ammonia solution were from Aldrich (Milwaukee, WI, USA). Dulbecco's modified Eagle's medium (DMEM), and fetal bovine serum (FBS) were from WelGENE (Daegu, South Korea).

2.2. Dye doped silica NPs

Two different kinds of dye (RITC and ICG) doped silica NPs were synthesized using the Stöber method [40]. RITC doped silica NPs were prepared following the literature method [39]. Briefly, after adding 3.08 μL APTS to 1 mL of 11 μM RITC solution, the mixture was vigorously stirred for 17 h. Next, 8.4 mL of ethanol and 622 μL ammonia solution were added to the mixture and the activation reaction was allowed to continue for 2 h at room temperature. After that, 355 μL TEOS was added and the mixture was stirred for 24 h at room temperature. This mixture was centrifuged at 4000*g* for 20 min, the supernatant was discarded, and the pellet of RITC doped silica NPs was resuspended in ethanol. These washing steps were repeated three times. Then, RITC doped silica NPs were dispersed in PBS solution and kept in the dark at 4° C.

ICG doped silica NPs were prepared as follows. First, given molar amounts of ICG and one of the three PEI solutions were added to 2 mL DMSO. The mixture was vigorously stirred for 1 h. Next, 8.4 mL of ethanol and 1.0 mL of ammonia solution were added to the mixture and the activation reaction was allowed to continue for 2 h. Then 355 μL TEOS was added and stirred for 24 h at room temperature. This reaction led to the formation of ICG doped silica NPs. This mixture was centrifuged at 4000*g* for 20 min. The NPs were then resuspended in ethanol. These washing steps were repeated three times. Finally, about 110 mg of ICG doped silica NPs were obtained. The resulting ICG doped silica NPs were dispersed in PBS solution and kept in the dark at 4° C. The supernatant solutions from the washing process were collected for the spectrophotometric estimation of ICG dye molecules not doped in the silica NPs.

The morphology of the NPs was examined under a transmission electron microscope (TEM, H-7600, Hitachi, Tokyo, Japan). Their sizes were assessed using public domain software Image J (NIH, Bethesda, MD, USA). The hydrodynamic sizes of NPs were measured using a dynamic light scattering (DLS) instrument (BI-200SM, Brookhaven, Holtsville, NY, USA). The absorbance and fluorescence spectra of ICG dye and ICG doped silica NPs were measured with a spectrophotometer (S3130, Scinco, Seoul, Korea) and a fluorescence spectrophotometer (Varian, Palo Alto, USA), respectively.

2.3. Photostability of free ICG dye and ICG doped silica NPs

ICG (2 mg/mL) and ICG doped silica NPs (2 mg/mL) in PBS were prepared in a 2 mL glass cell, and placed in a dark box, 40 cm below a UV lamp. The intensity of the UV light on the sample, measured by a power meter (10A-P; OPHIR Optronics, Danvers, MA, USA), was 12 mW/cm^2. The samples were exposed for 7 h. The fluorescence intensity was measured every 60 min using the fluorescence spectrophotometer.

2.4. Dye leakage from silica NPs

For each of the three kinds of ICG doped NPs, 5 samples of 10 mg NPs dispersed in 2 mL PBS by sonication were prepared. After measuring the initial absorbance, the 5 samples were kept in the dark at 37 °C. After 24 h, the NPs were centrifuged at 4000*g* for 20 min. The supernatant was discarded, and the pellet of ICG doped silica NPs was resuspended in PBS solution. Then, the fluorescence signal of the ICG doped NP solution was measured. This procedure was repeated four more times at intervals of 24 h.

2.5. Cell viability assay

The cell viability was assessed using a CCK-8 cell counting kit (Dojindo, Rockville, MD, USA) [44]. HEK293, a human embryonic kidney cell line, and HeLa, a human cervical cancer cell line, were cultured in DMEM, supplemented with 10% FBS, penicillin, and streptomycin at 37° C in a humidified atmosphere containing 5% CO_2. Individual wells of a 96-well microculture plate were filled with 1–5 $\times$ 10^3 cells/100 μL of the suspension of HEK293 or HeLA cells, and incubated with 0.1–0.8 mg/mL of three different silica NPs in a humidified incubator with 5% CO_2 for 24, 48 and 72 h at 37 °C. Afterwards 10 μL of the cell count solution of CCK-8 was added to each well, and incubated in a CO_2 incubator for 4 h. Absorbance at 450 nm was measured to determine the cell viability using a microplate reader (Bio-Rad Laboratories, Hercules, CA, USA). All the experiments were done in triplicate.

2.6. Tissue transmittance of NIR fluorescence from ICG doped silica NPs and RITC doped silica NPs

Fluorescence images were obtained using a Maestro In Vivo Imaging System (CRi, Woburn, MA, USA) for data acquisition and analysis. 0.1 mL of RITC doped silica NPs (10 mg/mL) or ICG doped silica NPs (10 mg/mL) was placed in a central well of a 96-well plate (well-diameter of 0.7 cm). Porcine muscles of thickness 1.0 cm, 1.5 cm, or 2.0 cm were fixed thereon. For RITC fluorescence image acquisition, the spectral imaging system was used with a 445–490 nm band pass filter and a 500–720 nm long pass filter for excitation and emission, respectively. The intensity of the blue excitation light at the sample surface was 8 mW/cm^2 and the exposure time was 5000 ms. For ICG fluorescence image acquisition, the spectral imaging system was used with a 710–760 nm band pass filter and a 780–950 nm long pass filter for excitation and emission, respectively. The intensity of the NIR excitation light at the sample surface was 8 mW/cm^2. The exposure time was 5000 ms.

3. Results and discussion

Since ICG is an amphiphilic molecule, having two polycyclic parts imparting a lipophilic character and a sulfonate group bound to each polycyclic part imparting a hydrophilic character to the molecule (Fig. 1a), ICG tends to form aggregates. When ICG is aggregated, self-quenching of its fluorescence emission has

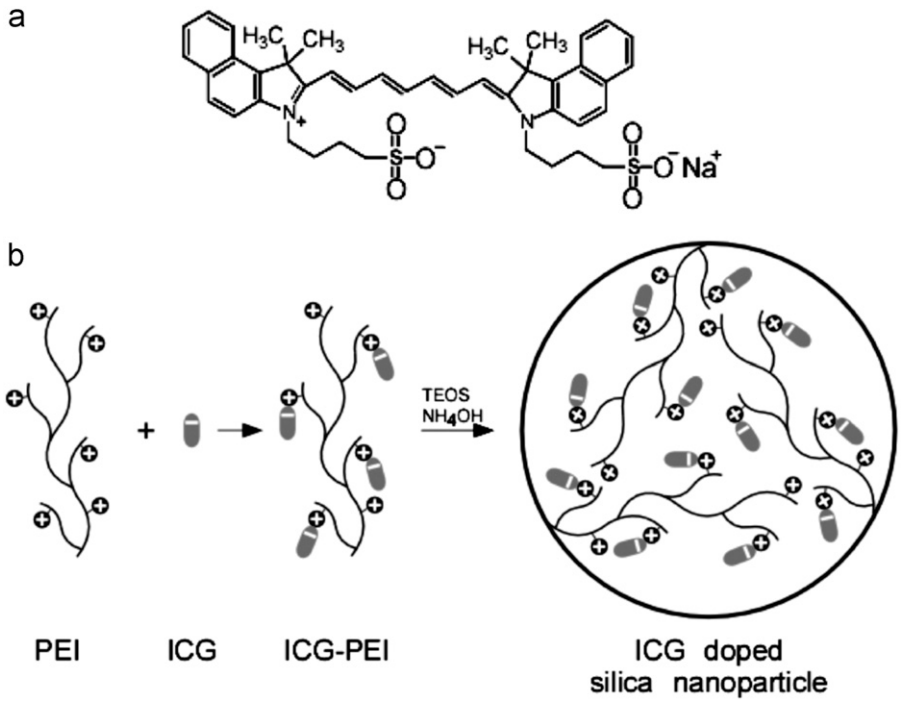

Fig. 1. (a) Indocyanine green and (b) Formation of ICG doped silica NPs is illustrated.

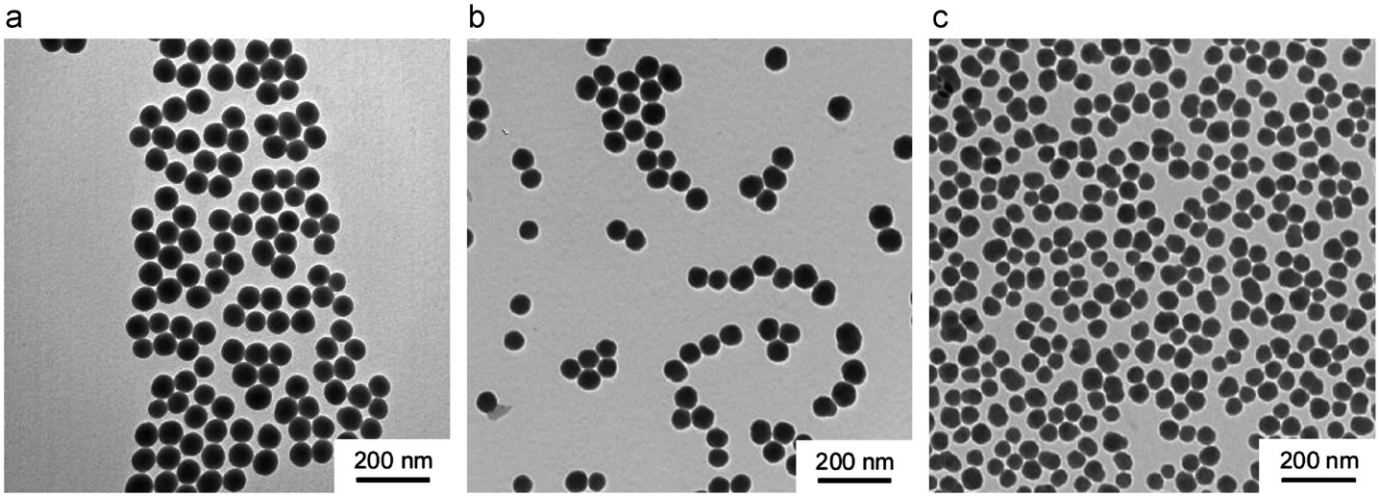

Fig. 2. TEM image of (a) ICG–PEI_{1200} doped silica NPs (60 ± 4 nm), (b) ICG–PEI_{10000} doped silica NPs (56 ± 5 nm) and (c) ICG–PEI_{60000} doped silica NPs (50 ± 5 nm). 1.0 mL of ammonia solution was used to catalyze the reaction.

been reported [18]. Accordingly, excessive localization of ICG by the formation of silica NPs may not be desirable. Moreover, since ICG is negatively charged [18,45], it is difficult for ICG molecules to be encapsulated by a negatively charged silica layer under neutral pH conditions due to electrostatic repulsion. The similar difficulty of synthesizing silica NPs doped with anionic dye Cy5 has been dealt with by conjugating the dye with biomolecules such as proteins or peptides [46]. We overcame this difficulty by ion-pairing ICG molecules with a positively charged polymer and then carrying out the self-assembly of the NPs by encapsulating them with a silica layer using the Stöber method. PEI is widely used in gene delivery and is positively charged in physiological pH conditions [47,48]. PEI was thus selected to ion-pair with the negatively charged sulfonate group of ICG to reduce the electrostatic repulsions between ICG and the silica matrix. In addition, the aggregation of ICG was prevented by this ion-paring with PEI, and thus self-quenching of the fluorescence emission was reduced. The formation of ICG doped silica NPs is illustrated in Fig. 1b.

3.1. Synthesis of ICG doped silica NPs

First, the amount of PEI in the synthesis of ICG doped silica NPs was optimized using various amounts of each of the three cationic PEI polymers (PEI_{1200}, PEI_{10000}, and PEI_{60000}) with 2 mg (2.6 μmol) of ICG in 2 mL of DMSO. When less than 10 nmol of PEI was used, the synthesis was rarely successful, probably due to insufficient neutralization of the negative charges of ICG. When more than 50 nmol PEI was used, particles of irregular and agglomerative shapes were obtained (Fig. S1 in Supplementary material). Between 10 and 50 nmol of PEI, ICG doped silica NPs were successfully synthesized. The size of NPs was mainly determined

by the amount of ammonia solution; the diameters increased from 50 to 200 nm as the amount of ammonia solution was increased from 1.0 to 2.0 mL (Fig. S2 in Supplementary material). There was no strong dependence of the NP sizes on the type of PEI. However, with PEI_{60000}, the synthesis was slightly more difficult. For example, when 1.0 mL of ammonia solution was used with PEI_{1200} or PEI_{10000}, silica NPs of 60 ± 4 nm or 56 ± 5 nm respectively were obtained with ease, in contrast to PEI_{60000} yielding only about 30% success rates with a size of 50 ± 5 nm (Fig. 2). When the amount of ammonia solution was increased to 1.4 mL, the synthesis using PEI_{60000} became as reliable as PEI_{1200} and PEI_{10000}. Note that it was difficult to obtain silica NPs smaller than 50 nm in diameter due to the limitation of the Stöber method [35]. The representative hydrodynamic sizes of the three ICG doped silica NPs obtained by DLS (Fig. S3 in Supplementary material) were in good agreement with those determined by TEM.

Next, for optimal fluorescence, the amount of ICG was varied from 0.5 mg (0.65 μmol) to 5.5 mg (7.1 μmol) with a fixed amount (20 nmol) of each type of PEI in 2 mL DMSO. There was no apparent dependence of the silica NP sizes on the amount of ICG. Fig. 3 shows the changes in fluorescence intensity of the ICG doped silica NPs with the amount of ICG. The fluorescence of ICG–PEI_{1200} silica NPs increased with the amount of ICG up to 1.5 mg, and then decreased rapidly afterwards. For ICG–PEI_{10000} silica NPs and ICG–PEI_{60000} silica NPs, maximum fluorescence was obtained with 2–3 mg of ICG. The decrease in fluorescence with the amount of ICG was attributable to self-quenching for high local concentrations of ICG [15]. The efficiency of loading ICG into silica NPs was also determined from the spectrophotometric estimation of ICG molecules in the supernatant solutions collected from the washing process, as described in Section 2.2. The loading efficiency was rather fluctuating and no clear trends with respect to the type of PEI or the amount of ICG were observed. For PEI_{1200}, PEI_{10000}, and PEI_{60000} the experimentally obtained loading efficiencies were 10–25%, 20–80%, and 35–50%, respectively (Fig. S4 in Supplementary material for the loading efficiency of ICG–PEI_{10000} doped silica NPs). In comparison, the efficiencies for the ICG entrapment of ICG doped PLGA NPs [27] and ICG doped NACs [31] were 1–74% and 34–97%, respectively.

3.2. Characteristics of ICG doped silica NPs

The photostability of ICG doped silica NPs was investigated. When a solution of (2 mg/mL) free ICG dye molecules was exposed to UV light of 12 mW/cm^2 for 7 h, the emission intensity decreased by as much as 72%. In contrast, the decrease was only about 7–17% for the (2 mg/mL) ICG doped silica NPs (Fig. 4a). Thus the photostability of ICG molecules in silica NPs was clearly improved compared to free ICG molecules in solution. The stability of the ICG doped silica NPs in a biologically relevant

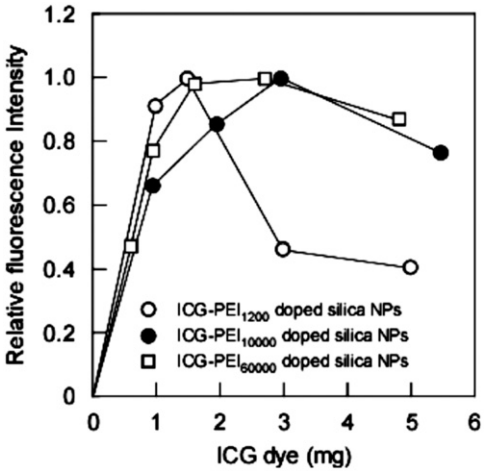

Fig. 3. Fluorescence intensity change of ICG doped silica NPs according to the initial amount of ICG that is ion-paired with 20 nmol of PEI_{1200}, PEI_{10000} and PEI_{60000}.

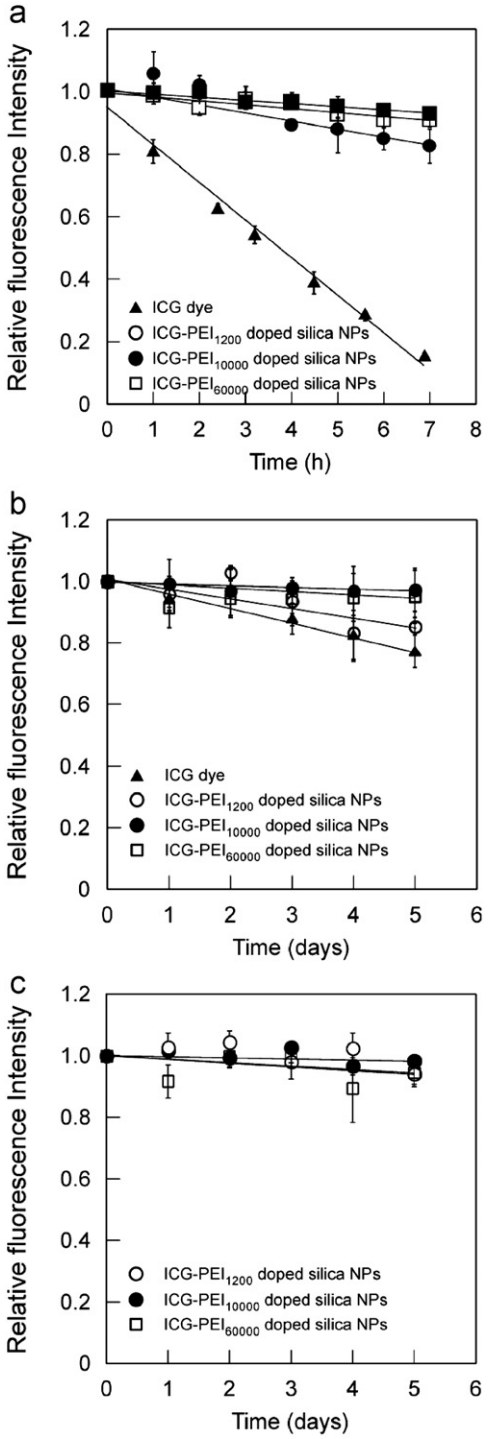

Fig. 4. (a) Photobleaching of 2 mg/mL ICG dye and ICG doped silica NPs. The samples were exposed to UV light. (b) Fluorescence intensity change of ICG dye and ICG doped silica NPs dispersed in DMEM with 10% FBS in the dark at 37 °C. (c) Dye leakage from silica NPs. Fluorescence intensity change of 5 mg/mL ICG doped silica NPs stored at 37° C in the dark. Bars represent the standard deviations ($n \geq 5$).

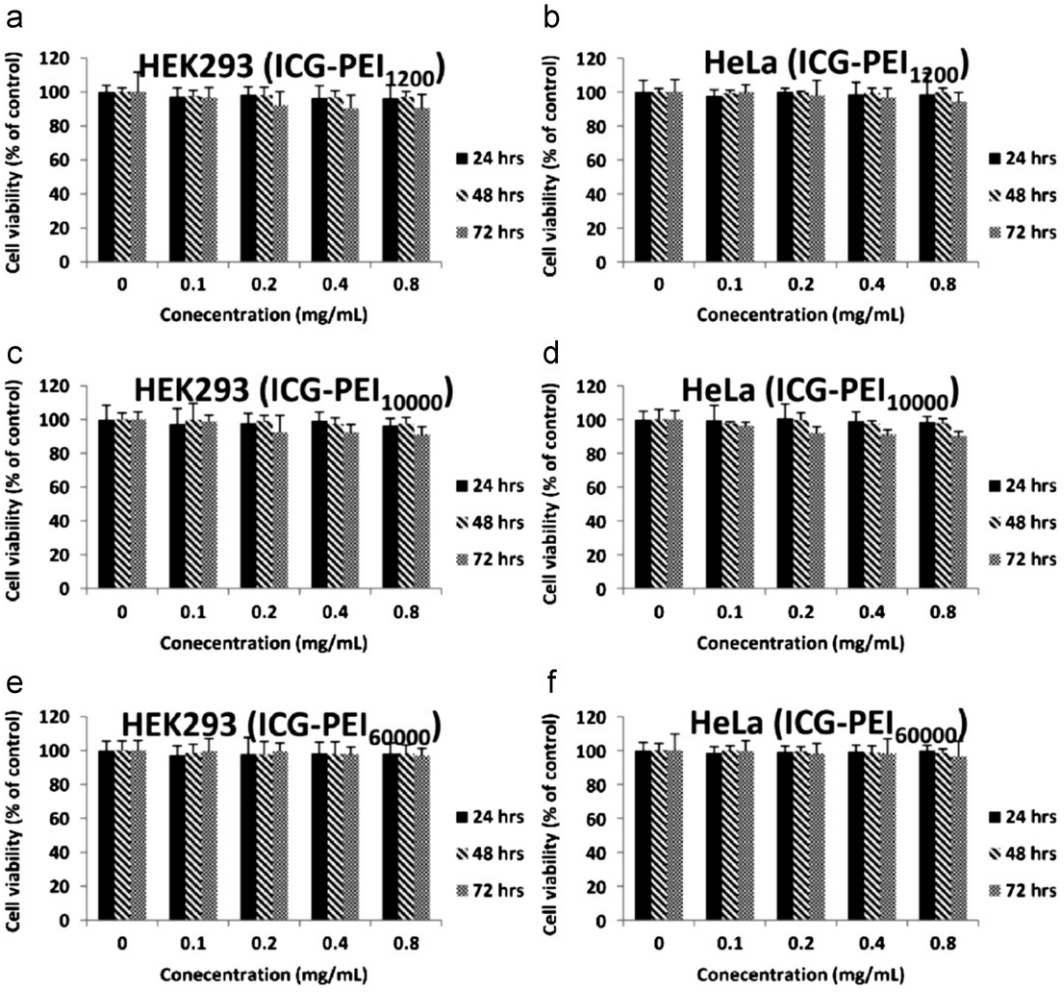

Fig. 5. HEK293 (a, c, e) and HeLa (b, d, f) cells were incubated with different amounts of the three ICG-PEI doped silica NPs for 24, 48 and 72 h. The results are presented as the percentage absorbance relative to control cells incubated in a probe-free medium. Data are expressed as mean ± SD of three independent experiments.

solution was also investigated. For the samples dispersed in DMEM with 10% FBS and stored in the dark at 37 °C, their fluorescence intensities and hydrodynamic sizes were monitored for 5 days. As shown in Fig. 4b, the fluorescence intensity decreased 2–4% for the ICG–PEI_{10000} and ICG–PEI_{6000} doped silica NPs, and 13% for the ICG–PEI_{1200} doped silica NPs while the intensity decreased about 22% for the ICG dye in 5 days. The hydrodynamic sizes did not show significant changes in 5 days (Table S1 in Supplementary material). Thus the ICG doped silica NPs were also stable in a biologically relevant solution.

The leakage of ICG molecules from silica NPs was also examined. Fig. 4c shows the changes in fluorescence from ICG doped silica NPs kept in PBS. Over 5 days, decreases of only 3–6% were observed. Compared to ~70% and 17% decreases in 8 h, respectively, for the ICG doped PLGA NPs [27] and ICG doped NACs [31], our ICG doped silica NPs showed dramatic improvements in reducing dye leakage.

According to the result, when ICG doped silica NPs were synthesized using the three types of PEI, all can reduce self-quenching of ICG and have high stability. They also showed a similar effectiveness in reducing dye leakage. However, the success rates of synthesizing ICG–PEI_{60000} silica NPs as small as 50 nm in diameter were poor, compared with those of ICG–PEI_{1200} silica NPs and ICG–PEI_{10000} silica NPs. In addition, ICG–PEI_{10000} doped silica NPs stopped self-quenching and photobleaching more effectively than ICG–PEI_{1200} doped silica NPs.

3.3. Cell viability studies

Fig. 5 shows the cell viability of HEK293 and HeLa cells incubated with the three different ICG–PEI doped silica NPs. The differences in cell viabilities after 24, 48 and 72 h of incubation were negligibly small, showing little cytotoxicity at concentration of 0.1–0.8 mg/mL. These observations suggest that the ICG–PEI doped silica NPs have good biocompatibility.

3.4. Tissue transmittance of NIR fluorescence from ICG doped silica NPs

The absorption and fluorescence spectra of the ICG doped silica NPs comprising of all the three PEIs were similar to those of ICG molecules, having excitation and emission maximum in the NIR region of 790 nm and 820 nm, respectively. As a demonstration of the advantage of NIR light having high transmittance into deep tissue [1,2], fluorescence images from the two types of dye (ICG and RITC) doped silica NPs passing through the porcine muscle were compared, as shown in Fig. 6. RITC doped silica NPs showed poor transmission and their fluorescence images were indiscernible from autofluorescence images arising from the tissue in the visible region (Fig. 6d). In addition, high concentration of pure ICG dye showed low fluorescence intensity because of self-quenching (Fig. S5 in Supplementary material). By contrast, NIR fluorescence from ICG-PEI_{10000} doped silica NPs was clearly observed (Fig. 6a).

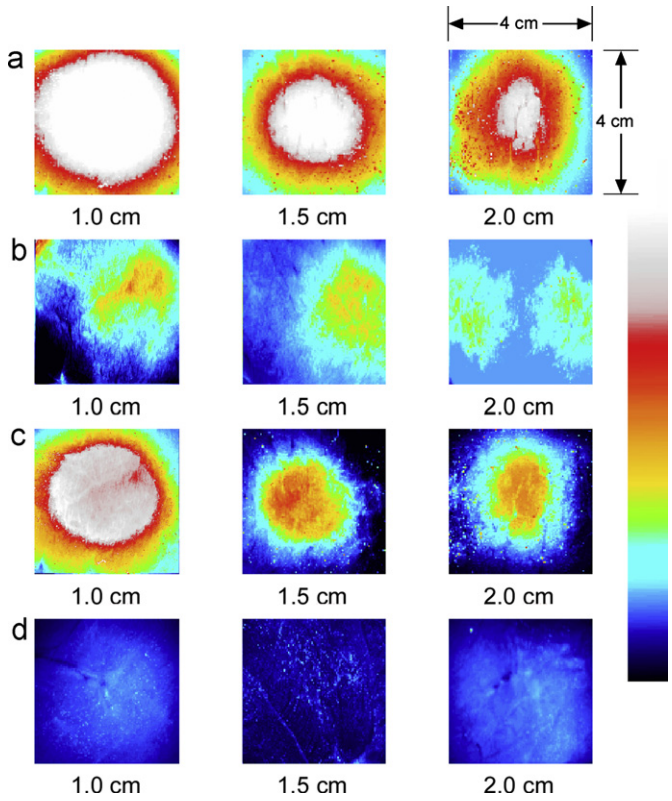

Fig. 6. (a) Fluorescence images of ICG doped silica NPs beneath porcine muscle with a 300 W xenon lamp, λ_{ex}=710–760 nm band pass filter with λ_{em}=780–950 nm long pass filter. (b) Fluorescence images of porcine muscle with a 300 W xenon lamp, and λ_{ex}=445–490 nm band pass filter and λ_{em}=500–720 nm long pass filter. (c) Fluorescence images of ICG doped silica NPs beneath porcine muscle were subtracted from the background images of porcine muscle (Fig. 6b). (d) RITC doped silica NPs beneath porcine muscle with a 300 W xenon lamp, λ_{ex}=445–490 nm band pass filter and λ_{em}=500–720 nm long pass filter. The thickness of porcine muscle was 1.0 cm, 1.5 cm and 2.0 cm (5000 ms exposure). Side bar: pseudo-color lookup table. (For interpretation of the references to color in this figure legend, the reader is referred to the web version of this article).

Furthermore, the images were processed to reduce the contribution of autofluorescence from porcine muscles, especially from the surface. First, images obtained by illuminating the porcine muscle sample (without silica NPs below) with visible light (excitation at 445–490 nm and emission at 500–720 nm) and NIR light (excitation at 710–760 nm and emission at 780–950 nm) were compared. The two images showed similar patterns (Fig. S6 in Supplementary material) and the former visible image can be used for the image processing of the latter NIR image. After adjusting the amplitudes, the autofluorescence images (Fig. 6b) were subtracted from the NIR fluorescence images from the silica NPs below the porcine muscle. The contrasts of the processed images (Fig. 6c) showed a significant improvement over those of the non-processed images (Fig. 6a).

In this study, the NIR fluorescence of 1 mg ICG doped silica NPs in 0.1 mL PBS solution was easily transmitted through a 2.0 cm thick tissue sample. In addition, the sizes of ICG doped silica NPs were suitable for accumulation in cancerous tissues via an enhanced permeability and retention effect [49]. Moreover, the silica surface can be easily modified for multimode imaging applications and the ICG doped silica NPs have high photostability and negligible leakages of ICG dye compared to other ICG containing PLGA NPs [27–30] and ICG containing NACs [31,32].

4. Conclusions

By forming ion-pairs with cationic polymers PEI_{1200}, PEI_{10000} and PEI_{60000}, negatively charged ICG molecules were successfully encapsulated inside a silica layer by the Stöber method. In addition, the pairing with PEI reduced fluorescence quenching and leakage of ICG dye molecules. The isolation of ICG molecules from the surroundings by the silica layer greatly enhanced the photostability of ICG doped silica NPs. Due to their NIR properties, the ICG doped silica NPs showed high transmittance through a sample of porcine muscles compared to RITC doped silica NPs. Since the cell viability test shows that ICG doped silica NPs have good biocompatibility, they may be useful not only in biological studies but also in medical applications, replacing current fluorescent probes for in vivo imaging. Considering the photostability, dye leakage properties, and success rates of synthesis, the ICG–PEI_{10000} silica NPs are the most suitable for in vivo imaging applications among the three types of ICG–PEI doped silica NPs.

Acknowledgments

This work was supported by the Ministry of Education, Science and Technology in Korea (2011-000237).

Appendix A. Supporting information

Supplementary data associated with this article can be found in the online version at doi:10.1016/j.talanta.2012.05.069.

References

[1] R. Anderson, J. Parrish, J. Invest. Dermatol. 77 (1981) 13–19.
[2] W. Cheong, S. Prahl, A. Welch, IEEE J. Quantum Electron. 26 (1990) 2166–2185.
[3] E.M. Sevick-Muraca, J.P. Houston, M. Gurfinkel, Curr. Opin. Chem. Biol. 6 (2002) 642–650.
[4] M.A. Yaseen, J. Yu, M.S. Wong, B. Anvari, Opt. Express 16 (2008) 20577–20587.
[5] M.A. Yaseen, J. Yu, B. Jung, M.S. Wong, B. Anvari, Mol. Pharmacol. 6 (2009) 1321–1332.
[6] S. Fickweiler, R. Szeimies, W. Baumler, P. Steinbach, S. Karrer, A. Goetz, C. Abels, F. Hofstadter, J. Photochem. Photobiol. B 38 (1997) 178–183.
[7] F. Schütt, J. Fischer, J. Kopitz, F.G. Holz, Clin. Exp. Ophthalmol 30 (2002) 110–114.
[8] G. Taichman, P. Hendry, W. Keon, Tex. Heart Inst. J. 14 (1987) 133–138.
[9] E.I. Altınoglu, T.J. Russin, J.M. Kaiser, B.M. Barth, P.C. Eklund, M. Kester, J.H. Adair, ACS Nano 2 (2008) 2075–2084.
[10] W. Baumler, C. Abels, S. Karrer, T. Weiss, H. Messmann, M. Landthaler, R.M. Szeimies, Br. J. Cancer 80 (1999) 360–363.
[11] D. Bechet, P. Couleaud, C. Frochot, M.L. Viriot, F. Guillemin, M. Barberi-Heyob, Trends Biotechnol. 26 (2008) 612–621.
[12] B.M. Barth, E.I. Altinoglu, S.S. Shanmugavelandy, J.M. Kaiser, D. Crespo-Gonzalez, N.A. DiVittore, C. McGovern, T.M. Goff, N.R. Keasey, J.H. Adair, T.P. Loughran, D.F. Claxton, M. Kester, ACS Nano 5 (2011) 5325–5337.
[13] J.F. Florian Schütt, Jürgen Kopitz, Frank G Holz, Clin. Exp. Ophthalmol. 30 (2002) 110–114.
[14] K. Motomura, H. Inaji, Y. Komoike, T. Kasugai, S. Noguchi, H. Koyama, Jpn. J. Clin. Oncol. 29 (1999) 604–607.
[15] R. Benson, H. Kues, Phys. Med. Biol. 23 (1978) 159–163.
[16] V. Saxena, M. Sadoqi, J. Shao, J. Pharm. Sci. 92 (2003) 2090–2097.
[17] M.L. Landsman, G. Kwant, G.A. Mook, W.G. Zijlstra, J. Appl. Physiol. 40 (1976) 575–583.
[18] T. Desmettre, J.M. Devoisselle, S. Mordon, Surv. Ophthalmol. 45 (2000) 15–27.
[19] R. Simmons, R.J. Shephard, J. Appl. Physiol. 30 (1971) 502–507.
[20] S. Mordon, J.M. Devoisselle, S. Soulie-Begu, T. Desmettre, Microvasc. Res. 55 (1998) 146–152.
[21] K.J. Baker, Proc. Soc. Exp. Biol. Med. 122 (1966) 957–963.
[22] M.A. Yaseen, J. Yu, M.S. Wong, B. Anvari, Biotechnol. Prog. 23 (2007) 1431–1440.
[23] S. Mordon, T. Desmettre, J.-M. Devoisselle, V. Mitchell, Lasers Surg. Med. 21 (1997) 365–373.
[24] R. Philip, A. Penzkofer, W. Bäumler, R.M. Szeimies, C. Abels, J. Photochem. Photobiol. A 96 (1996) 137–148.

[25] T. Ishizawa, N. Fukushima, J. Shibahara, K. Masuda, S. Tamura, T. Aoki, K. Hasegawa, Y. Beck, M. Fukayama, N. Kokudo, Cancer 115 (2009) 2491–2504.
[26] B.E. Schaafsma, J.S.D. Mieog, M. Hutteman, J.R. van der Vorst, P.J.K. Kuppen, C.W.G.M. Löwik, J.V. Frangioni, C.J.H. van de Velde, A.L. Vahrmeijer, J. Surg. Oncol. 104 (2011) 323–332.
[27] V. Saxena, M. Sadoqi, J. Shao, Int. J. Pharm. 278 (2004) 293–301.
[28] V. Saxena, M. Sadoqi, J. Shao, J. Photochem. Photobiol. B: Biol 74 (2004) 29–38.
[29] V. Saxena, M. Sadoqi, J. Shao, S. Kumar, J. Biomed. Nanotechnol. 1 (2005) 168–175.
[30] V. Saxena, M. Sadoqi, J. Shao, Int. J. Pharm. 308 (2006) 200–204.
[31] J. Yu, M.A. Yaseen, B. Anvari, M.S. Wong, Chem. Mater. 19 (2007) 1277–1284.
[32] J. Yu, D. Javier, M.A. Yaseen, N. Nitin, R. Richards-Kortum, B. Anvari, M.S. Wong, J. Am. Chem. Soc. 132 (2010) 1929–1938.
[33] X. Zhao, R.P. Bagwe, W. Tan, Adv. Mater. 16 (2004) 173–176.
[34] J. Yan, M.C. Estévez, J.E. Smith, K. Wang, X. He, L. Wang, W. Tan, Nano Today 2 (2007) 44–50.
[35] Y. Piao, A. Burns, J. Kim, U. Wiesner, T. Hyeon, Adv. Funct. Mater. 18 (2008) 3745–3758.
[36] D. Napierska, L.C.J. Thomassen, V. Rabolli, D. Lison, L. Gonzalez, M. Kirsch-Volders, J.A. Martens, P.H. Hoet, Small 5 (2009) 846–853.
[37] K. Yu, C. Grabinski, A. Schrand, R. Murdock, W. Wang, B. Gu, J. Schlager, S. Hussain, J. Nanopart. Res. 11 (2009) 15–24.
[38] Y.S. Lin, C.L. Haynes, J. Am. Chem. Soc. 132 (2010) 4834–4842.
[39] Y.H. Jeon, Y.-H. Kim, K. Choi, J.Y. Piao, B. Quan, Y.S. Lee, J.M. Jeong, J.K. Chung, D.S. Lee, M.C. Lee, J. Lee, D.S. Chung, K.W. Kang, Mol. Imaging Biol. 12 (2010) 155–162.
[40] W. Stöber, A. Fink, Bohn, J. Colloid Interface Sci. 26 (1968) 62–69.
[41] L. Wang, W. Tan, Nano Lett. 6 (2006) 84–88.
[42] S.M. Moghimi, C.J.H. Porter, I.S. Muir, L. Illum, S.S. Davis, Biochem. Biophys. Res. Commun. 177 (1991) 861–866.
[43] A. Lavasanifar, J. Samuel, G.S. Kwon, Adv. Drug Deliv. Rev. 54 (2002) 169–190.
[44] M.H. Kim, H.K. Na, Y.-K. Kim, S.R. Ryoo, H.S. Cho, K.E. Lee, H. Jeon, R. Ryoo, D.H. Min, ACS Nano 5 (2011) 3568–3576.
[45] K. Sauda, T. Imasaka, N. Ishibashi, Anal. Chem. 58 (1986) 2649–2653.
[46] X. He, J. Chen, K. Wang, D. Qin, W. Tan, Talanta 72 (2007) 1519–1526.
[47] S.R. Forrest, B.B. Elmore, J.D. Palmer, Catal. Today 120 (2007) 30–34.
[48] A. Kichler, C. Leborgne, E. Coeytaux, O. Danos, J. Gene Med. 3 (2001) 135–144.
[49] I. Brigger, C. Dubernet, P. Couvreur, Adv. Drug Deliv. Rev. 54 (2002) 631–651.